Accretion History of Active Black Holes from Type 1 AGN

Eduardo S. Pereira[1] and Oswaldo D. Miranda[1]

Abstract Almost all galaxies have massive central black holes in their centers with masses typically ranging from $\sim 10^5$ to $\sim 10^9 M_\odot$. However, the origin and evolution of these objects and their connection with the hosting galaxies are not completely understood yet. In this work we analyze the mass accretion rate of supermassive black holes (SMBH's) and the mean Eddington ratio (MER) of type 1 AGN using data from the Sloan Sky Survey. For this purpose we improve the method for constructing the subsample of SMBH, taking into account the survey flux limit and the bias of the sample. It was observed that the mean bolometric luminosity of the active black holes can be represented by a function composed by a power law in mass and a like-Schechter function in redshift. Our results also show that both the mean Eddington ratio and the mass accretion rate are proportional to this function.

Keywords black hole physics — galaxies: active — galaxies: evolution — galaxies: nuclei — quasars: general

1 Introduction

There is strong evidence that nearly all galaxies contain supermassive black holes (SMBHs) in their centers, and that the evolution of the SMBH and its host galaxy are connected (see, e.g., Ferrarese & Merritt 2000). Basically, there are two different ways for SMBHs grow up: by accretion of matter (Soltan argument - Soltan (1982)) or by merging with other black holes. However, there are some uncertainties about the formation mechanisms and initial masses of the progenitors, or seeds, of these SMBHs (see, e.g. Volonteri 2010). On the other hand, some studies indicate that accretion and not the merging of black holes is the dominant process for growing the supermassive black holes we find at the centers of present-day galaxies (Shankar et al. 2010, 2009; Bertie & Volonteri 2008; Volonteri 2005; Marconi et al. 2004).

The Eddington ratio is an important element to study the evolution of SMBHs. It is associated with both the dynamic of accretion as with the balance between the gravitational force and the radiation pressure of the accretion disk. The mean Eddington ratio evolution, as a function of the redshift, has been described, for example, by Hopkins & Hernquist (2009) and Cao (2010). On the other hand, some works discuss the evidence that the evolution of the mean Eddington ratio is also a function of the mass of the central black hole (DeGraf et al. 2012; Trakhtenbrot & Netzer 2012; Kollmeier et al. 2006; Lusso et al. 2012; Kelly & Shen 2013). However, the real significance of the mean Eddington ratio is not clear yet.

A recent study (Fathi et al. 2013) using the Atacama Large Millimeter/sub-millimeter Array (ALMA), and based on the kinematic analysis of the dense molecular gas in the central 200 parsecs of the nearby galaxy NGC 1097, have shown a molecular and ionized gas infall $\sim 0.6\, M_\odot\, yr^{-1}$ at $100\, pc$ distance from the central SMBH of NGC 1097. This inflow corresponds to $\dot{M} \sim 0.066\, \dot{M}_{\rm Edd}$ onto the central black hole with a mass $\sim 1.2 \times 10^8 M_\odot$. Beyond this mechanism, which is associated with the accretion of matter around the black hole, a second mechanism has been discussed in the literature. It is associated with the possibility that SMBHs could grow up from the collapse of rapidly rotating supermassive stars that may have formed in the early Universe (Reisswig et al. 2013; Choi et al. 2013). However, if we concentrate the attention on the accretion processes, then the fraction of these black holes,

Eduardo S. Pereira and Oswaldo D. Miranda

[1]Divisão de Astrofísica, Instituto Nacional de Pesquisas Espaciais, Brazil, SP 12227-010

that are growing by accretion of matter, can be seen from the activity of distant quasars. In the local universe, we can find a similar result from the low luminosity active galactic nuclei (AGN).

Generally speaking, the mass density of the SMBHs (MDBH) is obtained from the quasar luminosity function - QLF (see, e.g, Small & Blandford (1992); Yu & Tremaine (2002); Merloni et al. (2004); Wang et al. (2006); Shankar (2009); Raimundo & Fabian (2009); Shankar et al. (2013)). However, previous models don't give a direct way to study the accretion process as a function of the black hole mass (nor the redshift). In particular, a more complete scenario including the accretion processes could be used, for example, to study the spin variation of the SMBHs in the cosmological context.

In this work, we present a new data mining process to construct a representative subsample of active SMBHs. The major advantage of the method presented here is related to the fact that the flux limit of the catalog is taken into account in a more accurate way. We consider the behaviors of the probability density function of the bolometric luminosity (PDFL) distribution of quasars for each bin of mass, of the central black hole, and redshift. To study the bias of the sample we considered a Monte Carlo method, known as Bootstrap method. We also present an original method for obtaining the mass accretion rate and the mean Eddington ratio as a function of the SMBH masses and of the redshift as well.

This work is organized as follows: In section 2 we present details of the sample and pre-processing of the observational data. Section 3 presents the new method to construct the subsample of SMBHs. In the Section 4 the study of the mass accretion rate and the mean Eddington ratio are presented. The last section presents the final remarks of this work. We consider standard cosmological model (ΛCDM) with $\Omega_b = 0.04$, $\Omega_m = 0.24$, $\Omega_\Lambda = 0.76$, $h = 0.73$.

2 The Data sample

In this work we use as data sample the Sloan Digital Sky Survey Data Release 7 (SSDS DR7) Quasar Catalog (Schneider et al. 2010), that contains 105,783 type 1 AGN (quasars) with luminosity greater than $M_i = -22.0$. In particular, we consider the catalog provided by Shen et al. (2011) - the SSDS DR7 Catalog of Quasar Properties. This catalog contains supplementary information like: the *full-width-at-half-maximum* (FWHM) of broad lines; central black hole masses (estimated using the FWHM); luminosity of broad lines as well as the bolometric luminosity of the quasars. In order to construct the mean Eddington ratio and to calculate the mass accretion rate is necessary a homogeneous quasar subsample. Thus, once calculated the Eddington ratio, we observed that some objects had values greater than 100. We considered these objects as outliers and they were excluded of our subsample. Then, the final subsample contains 57,496 objects with redshift from 0.03 up to 4.5.

In the Figure 1 is presented the Eddington ratio as a function of redshift[1]. The objects are plotted with different colors according to the specific range of mass. Fig. 1 represents the total subsample. Note that our Figure 1 is similar to Figure 16 of Trakhtenbrot & Netzer (2012).

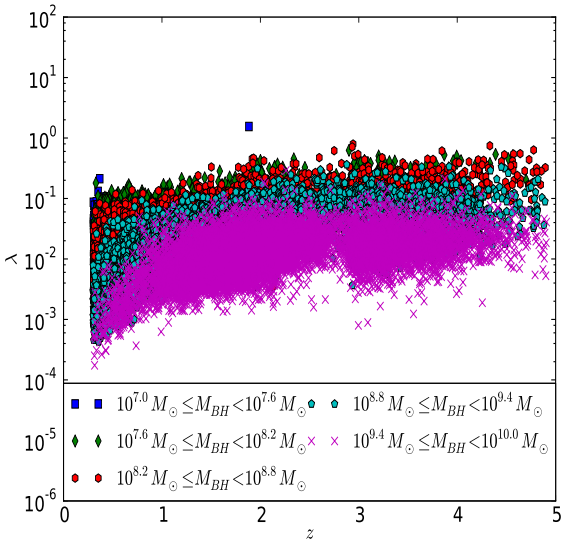

Fig. 1 The dimensionless quasar luminosity weighted by Eddington luminosity for all objects in our subsample.

3 Statistical Method

Concerning to statistical methods, there are some important points that must be taking into account (e.g. Kelly & Shen (2013)). Specifically they are: *i*) for a given mass, m_{bh}, there is a large range of luminosity, e.i., for a mass m_{bh} exists a bolometric luminosity distribution. This fact introduces statistical errors because some quasars are scattered above the flux limit; *ii*) statistical error in the virial mass produces more

[1]The Eddington ratio is obtained dividing the quasar bolometric luminosity by the Eddington luminosity, see eq. (7) for details.

quasars into bins of higher mass than lower mass when the BHMF declines toward higher values of m_{bh}. Another point is that no matter the method used, in some bins the amount of data may not be statiscally relevant.

In this section we present a method to take into account the points presented above. This is made in order to construct a representative and homogeneous subsample. The method consists in the following steps:

- The observational data are saved into a relational database;
- We perform a query into the database in order to select objects in a specific range of mass and redshift (binning process);
- if the amount of objects within a bin is lower than a fixed value, N_{min}, the bin is not considered;
- else, a new test is applied: this test consists in evaluating the probability density function of the bolometric quasar luminosity (PDFL) for the objects into the bin of mass m_{bh}, and for a given redshift. In this case, we consider the Freedman-Diaconis rule (Freedman & Diaconis 1981). This rule is used to determine the ideal width, w, of the histogram of PDFL, and it is given by:

$$w = 2\frac{IQR}{\sqrt[3]{N_{tot}}}, \quad (1)$$

  where IQR is the inter-quartile range and N_{tot} is the total number into the bin.
- if w is larger than a fixed value, the bin is not considered;
- else, the relevant informations are saved into a new table of the database.

Figure (2) presents a map in the space of $\log(m_{bh}) - z$. In this case was considered $w = \Delta log_{10}(L_b) = 0.1$ and $N_{min} = 30$. The map shows the bins with statistical representative amount of data. Note that, the sample is complete for our flux-limited criterion. However the incompleteness of the sample appears by the fact that a fraction of the objects (from a cut off of mass) are in a low activity regime and their luminosities are below of the flux limit of the catalog. The low activity regime can be observed in the Figure 1 for objects with relative low Eddington ratio ($\lambda \lesssim 10^{-1}$).

We observe that the objects with higher masses are dominant at distant redshifts. However, close to the present (low redshifts) the objects with lower masses become more actives, as expected. This result shows that our method is producing consistent results.

In the Figures 3, 4 and 5 are presented some examples of PDFL for $m_{bh} = 10^{8.5}\mathrm{M}_\odot$ and, $z = 0.3$, $z = 1.0$ and $z = 1.5$ respectively.

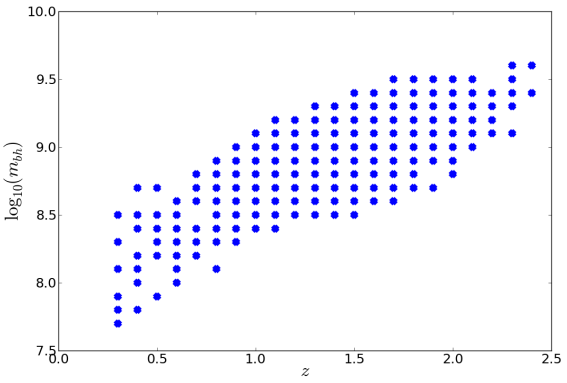

Fig. 2 Map of the binned space $\log(m_{bh}) - z$ with statistical representative amount of data.

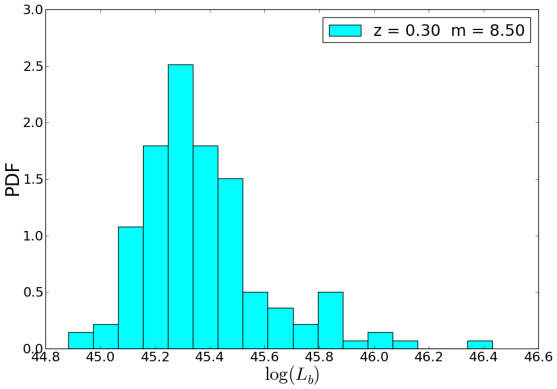

Fig. 3 Probability density Function estimator of the quasar luminosity distribution with central black hole mass of $10^{8.5}\mathrm{M}_\odot$ and $z = 0.3$.

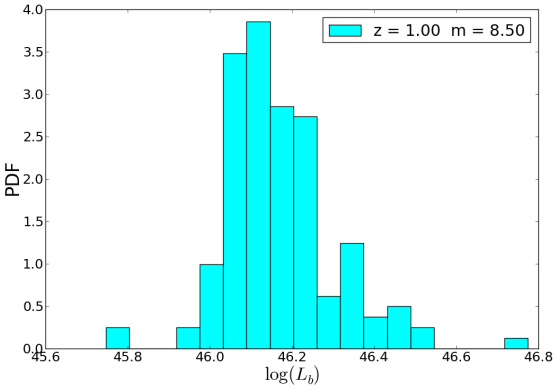

Fig. 4 Probability density Function estimator of the quasar luminosity distribution with central black hole mass of $10^{8.5}\mathrm{M}_\odot$ and $z = 1.0$.

To determine both the error and bias, caused by the facts presented at the beginning of this section,

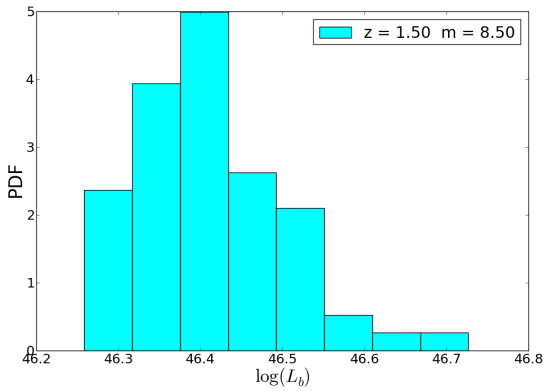

Fig. 5 Probability density Function estimator of the quasar luminosity distribution with central black hole mass of $10^{8.5}$M$_\odot$ and $z = 1.5$.

we adopted the non-parametric Monte Carlo bootstrap resample with replacement method (henceforward just bootstrap) (Wehrens et al. 2000; Carpenter & Bithell 2000; Press et al. 1992; Beran 1986; Wu 1986; Efron & Tibshirani 1986). The advantage of this method is that no prior knowledge about the data distribution is necessary. In the appendix A we present details about the bootstrap method. The bootstrap was used to calculate the errors of the mean bolometric luminosity, obtained from the data sample. Generally speaking, the bias was lower than 4 percent of the value of the mean bolometric luminosity. Also this method was used to determine the errors in the parameters of the likelihood function used to fit the data and as null hypothesis test.

To evaluate the goodness of the fittings, in this work was considered the adjusted coefficient of multiple determination, R$_a$-squared (Kutner et al. 2005):

$$R_a^2 = 1 - \left(\frac{n-1}{n-p}\right)\frac{SSE}{SSTO} \tag{2}$$

being:

$$SSE = \sum (f_i^{obs} - f_i^{esp})^2 \tag{3}$$

$$SSTO = \sum (f_i^{obs} - \bar{f}^{obs})^2 \tag{4}$$

where f_i^{obs} represents the data from the observations; f_i^{esp} is the expected value (theoretical value); $\bar{f}^{obs}$ is the mean value of the sample; n and p are the numbers of data and parameters respectively. The R$_a$-squared can have values between 0 and 1, and the result obtained can be interpreted as the percent of the data that lies in curve, or surface, fitted from the data. Values next to 1 indicate a good fit.

Note that as the number of faint sources decreases we observe that the width of the PDFL histograms become wider. In this case, not only the number of faint sources decreases but, in some bins, the total number of sources also decreases. The method present in this paper takes into account the reduction of the faint sources and also the reduction of the sources as a whole.

4 The Mean Mass Accretion Rate and The Mean Eddington Ratio

The bolometric luminosity of an accretion disk around a black hole is $L_b = \bar{\eta}\dot{M}_a c^2$, where c is the speed of light, $\bar{\eta}$ is the mean radiative efficiency and $\dot{M}_a = \dot{m}_{bh}/(1-\bar{\eta})$ is the mass accretion rate. On the other hand, the Eddington luminosity is related to the black hole mass, m_{bh}, by:

$$L_{edd} = \frac{c^2}{\tau_s} m_{bh}, \tag{5}$$

where $\tau_s = 4.2 \times 10^7$yr is the Salpeter time. The Eddington ratio is defined as:

$$\lambda \equiv \frac{L_b}{L_{edd}}, \tag{6}$$

that can be written as:

$$\lambda = \frac{L_b}{L_{edd}} = \frac{\tau_s}{c^2}\frac{L_b}{m_{bh}}, \tag{7}$$

or,

$$\lambda = \tau_s \frac{\bar{\eta}}{1-\bar{\eta}}\frac{\dot{m}_{bh}}{m_{bh}}. \tag{8}$$

From the method presented in the section 3, it is possible to construct a representative PDFL for each bin of mass and redshift. Thus, we define the mean Eddington ratio in terms of the mean bolometric luminosity as:

$$\bar{\lambda} \equiv \frac{\tau_s}{c^2}\frac{\bar{L}_b(z, m_{bh})}{m_{bh}}, \tag{9}$$

where $\bar{L}_b(z, m_{bh})$ is the mean value of the bolometric luminosity for a given bin of m_{bh} and z. From Eqs. (9) and (8), we write the mean mass accretion rate:

$$< \dot{m}_{bh} >= \frac{1}{c^2}\frac{1-\bar{\eta}}{\bar{\eta}}\bar{L}_b(z, m_{bh}). \tag{10}$$

In particular, we assume that $\bar{\eta}$ is constant with fiducial value 0.1. The data associated to $\bar{L}_b(z, m_{bh})$ are fitted by:

$$\bar{L}_b(m_{bh}, z) = \bar{L}_b^* \left(\frac{m_{bh}}{m_{bh}^*}\right)^{\alpha} \left(\frac{\tau_*}{t_u(z)}\right) \exp\left(-\frac{t_u(z)}{\tau_*}\right) \tag{11}$$

being $\bar{L}_b^*$, m_{bh}^*, α and τ_* free parameters and $t_u(z)$ is the look back time. The relation between the cosmic time and the redshift, for Cold Dark Matter (CDM) plus cosmological constant (Λ) model - (ΛCDM model), is given by (Pereira & Miranda 2010):

$$\left|\frac{dt_u}{dz}\right| = \frac{9.78 h^{-1} Gyr}{(1+z)\sqrt{\Omega_\Lambda + \Omega_m (1+z)^3}}. \tag{12}$$

The parameters are determined minimizing the following chi-square equation:

$$\chi^2 = \sum_{i=0}^{N} \sum_{j=0}^{M} \frac{\left[\bar{L}_{b,obs}^{ij} - \bar{L}_b(z^i, m_{bh}^j)\right]}{\sigma_{ij}}, \tag{13}$$

with σ_{ij} been the standard deviation of $\bar{L}_b$ in each bin.

In Table 4 we present the best fit parameters. The error and bias were obtained from 10000 bootstrap simulations. The adjusted coefficient of multiple determination were: $R^2 = 0.99$ for $\bar{L}_b$; $R^2 = 0.98$ for $\bar{\lambda}$; and $R^2 = 0.99$ for $< \dot{m}_{bh} >$. We tried different forms for the L_B function in order to fit the data. However, the choice of the Eq. (11) was based on the hypothesis test, using the bootstrap method. In some cases, the error and bias of the parameters become large. In other cases some parameters were out of the 95% percent of confidence level. Thus the final form of L_B was defined by the criteria of low error and bias, and that all parameters must be within 95% of confidence level.

In the Figure 6 is shown the mean bolometric luminosity as a function of black hole mass and redshift. The mean Eddington ratio and the mean accretion rate are plotted in the Figures 7 and 8. We observed that $\bar{L}_b$ increases for higher masses. However, the Eddington ratio picks at lower mass. These results can be explained by the fact that objects with low masses are younger than more massive objects. Thus, the dynamic of the processes associated with radiation and gravitation is more intensive for objects with low masses. Another important point is that the mean accretion rate declines when the redshift approaches to zero. This information can reflect the fact that, next to the present, occurs a reduction of the gas available for the growing of the black holes.

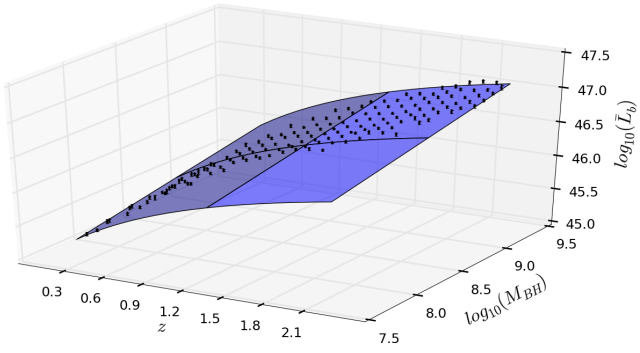

Fig. 6 Mean Bolometric Luminosity of type 1 AGN. The black dots were obtained from the data sample. The adjusted coefficient of multiple determination for this figure is $R^2 = 0.99$.

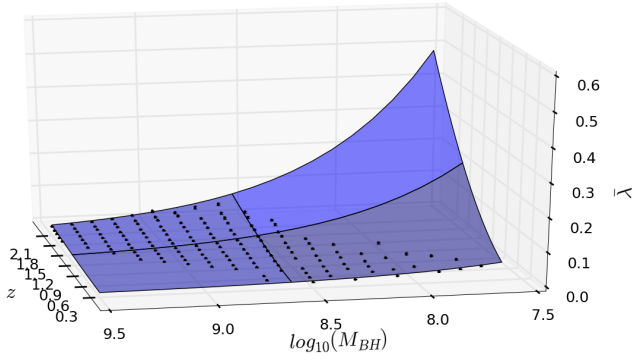

Fig. 7 Mean Eddington ration. The adjusted coefficient of multiple determination for this figure is $R^2 = 0.98$.

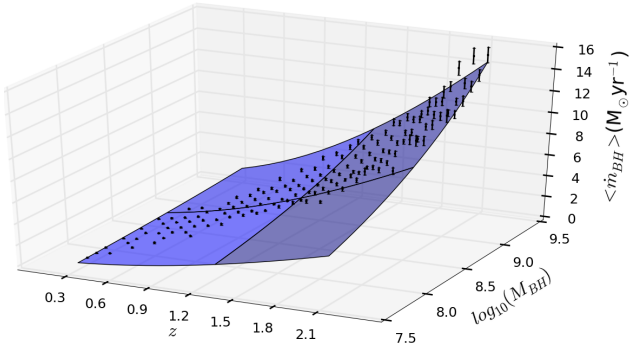

Fig. 8 Mean accretion rate. The adjusted coefficient of multiple determination for this figure is $R^2 = 0.99$.

Table 1 Best fit parameter: standard error, bias. All parameters are within 95% of confidence intervals. The values were obtained from 10000 Simulations.

	best fit	bias	error
L_b^*	3.05×10^{47}	6.65×10^{45}	3.14×10^{46}
m_{bh}^*	2.19×10^{11}	1.88×10^{10}	4.88×10^{10}
α	2.71×10^{-1}	-1.29×10^{-4}	1.18×10^{-2}
τ_*	4.81×10^{9}	1.05×10^{7}	1.69×10^{8}

5 Final Remarks

In this work we present a new method to obtain the mean Eddignton ratio and the mass accretion rate of supermassive black holes. The difference of our method, in relation to other described in literature, is that we employ a new data mining process in order to construct a representative subsample of the SMBHs. The major advantage of this method is the possibility of taking into account the catalog flux limit. This occurs because we consider the behaviors of the probability density function of the bolometric quasar luminosity distribution for each bin of mass, of the central black hole, and redshift. However, only a fraction of the original sample can be used to construct the final subsample. Here was considered as data sample the Sloan Digital Sky Survey Data Release 7 (SSDS DR7) Quasar Catalog (Schneider et al. 2010), that contains 105,783 type 1 AGN (quasars) with luminosity greater than $M_i = -22.0$. In particular, we consider the catalog provided by Shen et al. (2011) - the SSDS DR7 Catalog of Quasar Properties.

The mass accretion rate and the Eddington ratio are described in terms of the mean bolometric luminosity (MBL) as a function of both SMBH mass and redshift. The MBL, fitted from the data, increases in direction to high masses. However, the Eddington ratio picks at low mass. This result is explained by the fact that objects with low mass are younger than more massive objects. Thus, the accretion process is more intensive for objects with low mass. That is, at high redshifts we find a huge concentration of gas inside the halos not yet used for star formation. Thus, the black holes find, at high redshifts, favorable conditions for growing up. This last fact could be observed in the evolution of the mean accretion rate, that decreases for low redshift.

Acknowledgements ESP would like to thank the Brazilian Agency FAPESP (grant 2012/21877-5) for support. ODM would like to thank the Brazilian Agency CNPq for partial financial support (grant 304654/2012-4). We would also like to thank the referee which gave us a possibility to address several issues that were initially overlooked.

References

Beran, R., 1986, The Annals os Statistics, 14, 4, 1295.
Bertie, E., Volonteri, M., 2008, Astrophys. J., 195, L65
Cao, X., 2010, Astrophys. J., 725,388
Carpenter, J., Bithell, J., 2000. Statist. Med., 19,1141
Choi, J.-H., et al., 2013 (arXiv:1304.1369)
Conroy C., Wechsler R.H. 2009, ApJ, 696, 620
DeGraf, C., et al. 2012 Astrophys. J., 755 L8
Efron B., Tibshirani R., 1986, Statistical Science, 1, 54
Fathi, K., et al., 2013 (arXiv:1304.6722)
Fardal M.A., Katz N., Weinberg D.H., Davé R. 2007, Mon. Not. R. Astron. Soc., 379, 958
Ferrarese, L., Merritt, D. 2000,Astrophys. J., 539, L9
Franceschini A., Hasinger G., Miyaji T., Malquori D. 1999, Mon. Not. R. Astron. Soc., 310, L5
Freedman D., Diaconis P. 1981. Prob. Theory and Rel. Fields, 57, 4, 453
Haiman Z., Ciotti L., Ostriker J.P. 2004, Astrophys. J., 606, 763
Heckman T.M., Kauffmann G., Brinchmann J., Charlot S., Tremonti C., White S.D.M. 2004, Astrophys. J., 613, 109
Hopkins P.F. 2004, Astrophys. J., 615, 209
Hopkins P.F. 2007, Astrophys. J., 654, 1175
Hopkins A.M., Beacom J.F. 2006, Astrophys. J., 651, 142
Hopkins, P.F., Hernquist, L. 2009, Astrophys. J., 698, 1550
Kelly B. C., Merloni, A., 2012, Adv. in Astron., 2012, 21
Kelly B. C., Shen Y., 2013, Astrophys. J., 764, 45
Kollmeier, J. A., et al., 2006, Astrophys. J., 648,128
Kutner, M. H., et al. 2005. Applied linear statistical models. New York, NY: Mc-Graw-Hill Irwin. 5. 1396 p.
Li Y., Wang J., Ho L. C., 2012, Astrophys. J., 749, 187
Lusso, E., et al. 2012, Mon. Not. R. Astron. Soc., 435,623
Mahamood A., Devriendt J.E.G., Silk J. 2005, Mon. Not. R. Astron. Soc., 359, 1363
Marconi, A., et al., 2004, Mon. Not. R. Astron. Soc., 351, 169
Merloni, A. 2004, Mon. Not. R. Astron. Soc., 353, 1035
Merloni A., Rudnick G., Di Matteo T. 2004, MNRAS, 354, L37
Page M. J., Carrera F. J., 2000, MNRAS, 311, 433
Pereira, E. S., Miranda, O.D., 2011, Mon. Not. R. Astron. Soc., 418,L30
Pereira E.S., Miranda O.D. 2010, Mon. Not. R. Astron. Soc., 401, 1924
Press, W. H., et al., Numerical Recipes in Fortran 77, Vol. 1, 2nd edn. (Cambridge University Press, Cambridge, 1992), p. 948.
Raimundo, S. I., Fabian, A. C. 2009, Mon. Not. R. Astron. Soc., 396, 1217
Reisswig, C., et al., 2013 (arXiv:1304.7787)
Shankar F. 2009, New Astron. Rev., 53, 57
Shankar F., Weinberg D.H., Miralda-Escude J. 2009, Astrophys. J., 690, 20
Shankar F., et al. 2010, Astrophys. J., 718, 213
Shankar F., Weinberg D.H., Miralda-Escude ' J. 2013, Mon. Not. R. Astron. Soc., 428, 421
Shen, Y., et al., 2011, Astrophys. J.Supplement Series, 194:45 (21pp), 2011 June
Schneider, D. et al., 2010, Astron. J., 139, 6, 2360
Small. T.A., Blandford R.D. 1992, MNRAS, 259, 725
Soltan, A. 1982, Mon. Not. R. Astron. Soc., 200, 115s
Springel V., Hernquist L. 2003, MNRAS, 339, 312
Trakhtenbrot, B. and Netzer, H. 2012, Mon. Not. R. Astron. Soc., 427, 3081
Vestergaard, M., et al., 2008, Astrophys. J., 674, L1
Volonteri, M., et al., 2005, Astrophys. J., 667, 704
Volonteri, M., 2010, Annu. Rev. Astron. Astrophys., 18, 279
Wang, J., Chen, Y., Zhang, F. 2006, Astrophys. J., 647, L17
Wehrens, R., et al. 2000, Chem. and Intel. Laborat. Sys., 54, 35.
Wu, C. F. J., 1986. The Ann. of Stat., 14, 4, 1261.
Yu, Q., Tremaine, S. 2002, MNRAS, 335, 965

This manuscript was prepared with the AAS LaTeX macros v5.2.

A The Bootstrap Method

The Monte Carlo Bootstrap method (henceforward bootstrap method) is a powerful tool to obtain the bias, standard error and percentile confidence level interval of the parameters considering statistical inferences from data resampling (Wehrens et al. 2000; Carpenter & Bithell 2000; Beran 1986; Wu 1986; Efron & Tibshirani 1986). In general, there are two bootstrap methods, the parametric and the non-parametric.

In the parametric bootstrap, one fits a plausible model to the data and acts thereafter as though the fitted model is true (Beran 1986). In this case, new samples are obtained, randomly, from the fitted model, and these new data are assumed as the bootstrap resample. This is an interesting method for low number of original data.

In this work we consider the non-parametric bootstrap method. This method consists in creating new samples from the original data. The new bootstrap sample is obtained by random selection of objects from the original data, being that the new sample has the same size as the original sample (Wehrens et al. 2000; Carpenter & Bithell 2000; Press et al. 1992). About 30 percent of new samples are constituted by repeated objects (Press et al. 1992). Note that, this could produce a slight modification to the statistical properties of the binned sample. However, it is possible to test the sensibility of the parameters with respect to the distribution and completeness of the original sample. To do that, we developed a module using Python language, called pybootstrap, that is released under GNU general license version 3. It can be downloaded from http://github.com/duducosmos/pyboostrap. The general idea of the bootstrap method is present hereafter.

Let θ be a parameter of a population. From a random sample $(X_1, X_2, ..., X_n)$, with length n sufficiently large, we have a statistical correspondent parameter $\hat{\theta}$. Note that $\hat{\theta}$ is an estimator of θ.

The bias, $bias_{B,i}$ and the standard error, $se_{B,i}$, of the i parameter obtained from the bootstrap method are (Wehrens et al. 2000):

$$bias_{B,i} = \hat{\theta}^*_{.i} - \hat{\theta}_i, \tag{A1}$$

$$se_{B,i} = \sqrt{\frac{1}{B-1}\sum_j \hat{\theta}^*_{ij} - \hat{\theta}^*_{.i}} \tag{A2}$$

where $\hat{\theta}_i$ is the ith parameter, $\hat{\theta^*_{.i}}$ is the mean value of the ith parameter calculated from the bootstrap subsamples. The $\hat{\theta}^*_{ij}$ is the jth bootstrap parameter correspondent to ith parameter obtained from the original sample and B is the total number of bootstrap samples. The percentile bootstrap confidence interval is calculated as follows: first, the parameters r^{i*} are drawn, and, sorted in crescent way, from the bootstrap sample. Then, the α-percentile interval confidence level is (Wehrens et al. 2000):

$$r^{i*}_{(B+1)\alpha/2} \leq \theta_i \leq r^{i*}_{(B+1)(1-\alpha/2)}. \tag{A3}$$

The principal question solved by the bootstrap method is how accurated $\hat{\theta}$ is as an estimator of θ (Efron & Tibshirani 1986). Nowadays, with relatively low cost of powerful computers, the bootstrap method became a very useful and robust statistical tool to study a large quantity of observational data.